Characteristics of pre-sensitization-related acute antibody-mediated rejection in a rat model of orthotopic liver transplantation

Yuanyi Mang[1]#, Shengning Zhang[1]#, Jiaojiao Zhao[1], Jianghua Ran[1], Yingpeng Zhao[1], Laibang Li[1], Yang Gao[1], Wang Li[1], Guoyu Chen[1], Jun Ma[1], Li Li[1], Fukai Bao[2]

[1]Department of Hepato-Biliary-Pancreatic Surgery and Liver Transplantation Center, the Calmette Affiliated Hospital of Kunming Medical University, the First People's Hospital of Kunming, Clinical Medical Center for Organ Transplantation of Yunnan Province, Kunming, China; [2]Department of Pathogen Biology and Immunology, Faculty of Basic Medical Science, Kunming Medical University, Kunming, China

Contributions: (I) Conception and design: Y Mang, S Zhang, Li Li; (II) Administrative support: Li Li, J Ran; (III) Provision of study materials or patients: F Bao, Y Zhao; (IV) Collection and assembly of data: J Zhao, La Li, Y Gao; (V) Data analysis and interpretation: W Li, G Chen, J Ma; (VI) Manuscript writing: All authors; (VII) Final approval of manuscript: All authors.

#These authors contributed equally to this work.

Correspondence to: Li Li. Department of Hepato-Biliary-Pancreatic surgery and Liver Transplantation Center, the Calmette Affiliated Hospital of Kunming Medical University, the First People's Hospital of Kunming, Clinical Medical Center for Organ Transplantation of Yunnan Province,1228 Beijing Road, Kunming, Yunnan, China. Email: ynkmlili62@hotmail.com; Fukai Bao. Department of Pathogen Biology and Immunology, Faculty of Basic Medical Science, Kunming Medical University, 1168 Chunrong West Road, Kunming 650500, Yunnan, China. Email: baofukai@kmmu.edu.cn.

Background: To establish an animal model of pre-sensitization following liver transplantation either with or without immunosuppressors. To study whether accelerated liver rejection or acute antibody-mediated rejection (AMR) occurred and study the characteristics and potential mechanism in the animal model.

Methods: Lewis (LEW) rats were subjected to liver [liver graft of Brown Norway (BN) rat] transplantation 2 weeks after lymphocyte injection (lymphocytes of BN rat; pre-sensitization). At 2 weeks after transplantation, serum samples of recipients were collected for antibody analysis to identify donor-specific alloantibody (DSA) level. The recipients were treated with or without a low dose of immunosuppressor (2 mg/kg). The liver grafts of each group were analyzed by hematoxylin and eosin (HE) stain, Masson stain, CK19, C4d, and CD20 immunohistochemical (IHC) stain, CD3, CD68, and CD86 immunofluorescence and transmission electron microscope (TEM) to study the characteristics of liver rejection. Moreover, cytotoxin-associated genes, M1 macrophages conversion-related proteins, and interleukin-6 (IL-6) signaling pathway proteins were detected by western blotting.

Results: High level of DSA and accelerated liver rejection occurred in the pre-sensitized rat models following liver transplant. Accelerated liver graft rejection occurred in the pre-sensitized, post liver transplant rats regardless of whether a low dose immunosuppressor had been applied. Severe injury of the interlobular bile ducts and accelerated fibrosis could be observed. Moreover, evidence of endothelial injury, such as capillary inflammation, was found in the pre-sensitized, post-transplant rats. In addition, C4d deposition and M1 macrophages recruitment were also found in this sensitized followed transplant model, indicating that complement activation might occur in this model. The levels of IL-6, JAK1, STAT3, SHP2, and ERK1-2 were increased in the pre-sensitized, post-transplant rats.

Conclusions: Pre-sensitized post liver transplant rats might be potential AMR models for further study.

Keywords: Donor-specific alloantibody (DSA); antibody mediated rejection; liver transplantation; rat

Introduction

In recent years, there have been reports of donor-specific alloantibody (DSA)-associated liver graft rejection (1). The DSAs have been related to high risks of early acute rejection and death. *De novo* DSAs have been related to chronic rejection, graft fibrosis, and dysfunction (1). Poor prognosis of recipients with high levels of DSA has been related to antibody-mediated rejection (AMR) (2,3). Diagnosis and treatment of AMR in liver transplant are difficult. The diagnosis of AMR in a liver graft is different from that of the kidneys due to the abundant blood flow and Kupffer cells (2,4), which make C4d deposition more difficult to detect in liver graft biopsy. Thus, the diagnostic criteria of liver graft AMR were confirmed in the 2016 comprehensive update of the Banff Working Group (5). The new criteria focused on endothelial injury and micro vessel inflammation. Reasonable exclusion of other insults that might cause a similar graft injury was also deemed important for diagnosis of AMR (5). AMR can be divided into acute AMR and chronic AMR. Acute AMR occurs most commonly in the first 2 weeks after transplantation. Acute AMR presents with a delayed peak in aminotransferases, refractory thrombocytopenia, and resistance to steroid treatment. Acute AMR may lead to long-term outcomes, such as dysfunction of transplanted liver or chronic rejection, and etc. It can progress to graft failure if left untreated. Progressive, atypical fibrosis is the characteristic of chronic AMR. Class II DSA, most commonly against the DQ locus, is thought to cause the majority of chronic AMR (6). The mechanism of AMR in liver graft is still unclear, which makes treatment difficult. Pulse steroid therapy, intravenous immune globulin (IVIG), plasma replacement, increased dose of mycophenolate mofetil, rituximab, bortezomib, and tocilizumab have been presented as alternative treatment options (7-9). However, how to determine which therapy to apply and weigh the risk of infection according to diagnosis have been difficult because of the lack of clarity regarding mechanism. Moreover, microvascular inflammation, endothelial cell activation by electron microscopy, gene expression profile, and the design of therapeutic trials need to be explored in liver graft AMR. Thus, there is a need to establish an animal model with AMR with which to explore mechanisms (2).

Previous studies have used sensitized animal models (lymphocytes injection or transfusion before transplant) to explore accelerated rejection in solid organs (10,11). The plasma of sensitized rats had high levels of DSA, which might be related to AMR. In our study, we used Brown Norway (BN) rats as donors and Lewis (LEW) rats as recipients. Lymphocytes of BN rats were injected into LEW rats for sensitization before liver transplant. Accelerated liver rejection and evidence of AMR were found in this model. We have described the pathological characteristics, M1 macrophages recruitment, and activation of interleukin-6 (IL-6) signaling pathways in pre-sensitized liver transplant rats. We present the following article in accordance with the ARRIVE reporting checklist (available at https://atm.amegroups.com/article/view/10.21037/atm-22-4311/rc).

Methods

Animals

Male 10–12-week-old (250–300 g) LEW ($RT1^1$) and BN ($RT1^n$) rats were purchased from Beijing Vital River Laboratory Animal Technology Co., Ltd. (Beijing, China). All rats were maintained under specific-pathogen-free housing conditions at the Department of Laboratory Zoology, Kunming Medical University. Animal experiments were performed under a project license (No. kmmu20211208) granted by institutional review board of Kunming Medical University, in compliance with the institutional guidelines for the care and use of animals. A protocol was prepared before the study without registration. Liver grafts were procured from BN rats. The LEW rats as recipients were divided into 6 groups (at least 3 recipients in each group, n=3), as follows: (I) LEW control group: LEW rats which received no treatment; (II) sensitized group (S group): spleen of BN rat was cut into pieces and crushed on a cell strainer (40 μm) [Becton, Dickinson, and Co. (BD), Franklin Lakes, USA]. Filtered cells were lysed by erythrocyte lysate (Solarbio, Beijing, China) and then washed twice with Roswell Park Memorial Institute (RPMI)-1640 medium (Gibco, Waltham, MA, USA). Cell counting was performed with a hematocytometer. Then, 5×10^7 cells were re-suspended in 1 mL phosphate-buffered saline (PBS; Biosharp, Hefei, China) and injected into LEW rats by tail vein; (III) liver transplantation group (T group): a liver graft from BN rats was transplanted into LEW rat without any immunosuppressor; (IV) liver transplantation and pre-sensitized group (TS group): LEW rats underwent liver (liver graft of BN rat) transplantation 2 weeks after BN rat lymphocyte injection. At 2 weeks after transplantation, serum samples of recipients were collected for antibody

analysis to identify the DSA level. Recipients were treated without any immunosuppressors; (V) liver transplantation with immunosuppressor group (TI group): the liver graft from a BN rat was transplanted into a LEW rat with low dose of CsA (2 mg/kg/d, intragastric administration); and (VI) liver transplantation and pre-sensitization with immunosuppressor group (TITS) group: pre-sensitized LEW rats underwent liver transplantation as the TS group. Recipients were treated with low dose of CsA (2 mg/kg/d, intragastric administration) after transplantation. At 14 days after liver transplantation, recipients in each group were euthanized after collection of serum, splenic cells, and liver graft tissue.

Orthotopic transplant procedure

Liver graft procurement: the abdomen of a BN rat was opened under ether inhalation anesthesia. The ligaments around liver were disassociated. An injection of 50 U heparin sodium was administered at the iliac vein bifurcation. Then, a 4F (1.3 mm diameter) capillary plastic pipe was trimmed to an 8 mm length as a stent for common bile duct. The stent was inserted into common bile duct and fixed. After abdominal aortic puncture, 30 mL 4 ℃ lactated Ringer's solution (heparin sodium 25 U/mL, dexamethasone 0.01 mg/mL) was perfused through the aorta. Meanwhile, the vena cava was cut open to drain venous blood. The upper and lower segments of the retrohepatic inferior vena cava and portal vein were cut.

Stent fixation for the vena cava and portal vein: the liver graft of the BN rat was moved to a dish with 4 ℃ lactated Ringer's solution on ice. A 9F (3 mm diameter) capillary plastic pipe was trimmed to a 5 mm length as a stent for portal vein. Then, a 12F (4 mm diameter) capillary plastic pipe was trimmed to 5 mm in length as a stent for the lower segments of the retrohepatic inferior vena cava. The stents were inserted into these vessels and fixed using 5-0 prolene ligation (the intima of the vessel at ligation was everted).

Transplant: the LEW rat was fixed on an animal console under ether inhalation anesthesia. The ligaments around the liver were disassociated. The portal vein and common bile duct were exposed, ligated, and cut. Vascular blocking clamps were used to clamp the recipient part of the portal vein and bile duct. The recipient part of the 6 mm length portal vein and bile duct were reserved. The upper and lower segments of the retrohepatic inferior vena cava were clamped. The liver of the recipient was moved outside abdomen. The dorsum of the recipient rat was bulked with

a 50 mL syringe tube for easy suturing. The liver graft was placed after an ice cotton ball had been placed in the abdominal cavity. The upper segments of the retrohepatic inferior vena cava and recipient's vena cava were joined by suturing using 8-0 prolene. The stent of the portal vein was inserted into the recipient's portal vein to maintain the ability of the recipient vessel to enclose the everted vessel of the donor and fixed by 6-0 prolene. The upper segments of the retrohepatic inferior vena cava and recipient's vena cava were joined in the same way. All clamps were loosened and 30 mL 40 ℃ saline solution was used to increase the temperature of the graft and abdominal cavity. The abdominal incision was closed after a hemostasis check. During the perioperative period, the antibiotic cefazolin was injected by tail vein for 7 days after transplantation.

DSA analysis and C4d analysis for recipients

The serum of LEW rats was collected for antibody analysis to identify the levels of immunoglobulin (IgG)1, IgG2a, IgG2b, IgG2c, and IgM by flow cytometry. Number of 1×10^6 splenic cells were diluted into 50 μL PBS and incubated with 200 μL 5% bovine serum albumin (BSA) (Sigma-Aldrich, St. Louis, MO, USA) for 30 minutes in 4 ℃ to block Fc receptor. The serum of LEW rats in each group were incubated with lymphocytes of rats respectively in room temperature for 1 hour. Mouse anti-Rat IgG1, IgG2a, IgG2b, IgG2c, and IgM (heavy chain) antibody [fluorescein isothiocyante (FITC) conjugate] (GeneTex, Irvine, CA, USA) as secondary antibodies were incubated with washed cells in 4 ℃. Flow cytometry (FC500; Beckman Coulter, Krefeld, Germany) analysis intensity of FITC to detect the DSA level. At 14 days after liver transplantation, splenic cells of LEW rats (recipients) were isolated and detected for C4d expression using rabbit anti-rat C4d (Cat. No. HP8034-100UG; Hycult Biotech, Beutelsbach, Germany) and goat anti-rabbit IgG Antibody (FITC conjugate) (Cat. No. AP132F; Millipore, Darmstadt, Germany). Flowjo software (BD, USA) was used for data analysis and graphic visualization.

Histopathology, C4d (C4d-score analysis), immunohistochemical (IHC) analysis, and Masson staining

Liver graft tissues in each group were fixed by formalin and embedded in paraffin. Tissues were cut into 4 μm slides. Slides were deparaffinized and treated by gradient xylene and ethanol for hematoxylin and eosin (HE) staining

(Solarbio, Beijing, China) and immunoperoxidase staining. Slides were viewed and photographed on a positive-mounted fluorescence microscope using the white light pattern (BX53F; Olympus, Tokyo, Japan). The rejection activity index (RAI) in each group was calculated from the 3 individual scores (portal inflammation, bile duct damage, and venular endothelialitis) (12). The AMR related histopathology (h)-score was calculated according to level of microvasculitis (5). Slides were put in a slide rack and placed in a glass beaker containing 500 mL of 0.01 M citrate buffer (Thermo Fisher, Walham, MA, USA) for antigen retrieval and then washed for immunostaining. The following items were used as primary antibodies: anti C4d (50^{-1} Cat. No. HP8034-100UG; Hycult Biotech, Germany), anti-cytokeratin 19 (200^{-1} Cat. No. ab220193; Abcam, Cambridge, UK), and anti CD20 (100^{-1} Cat. No. ab64088; Abcam, UK). A GTVision III universal anti-mouse/rabbit immunohistochemistry (IHC) kit (Cat. No. GK500705; Gene Tech, Shanghai, China) was used for secondary antibodies and chromogenic reagent. The C4d score in each group was calculated according to level of C4d deposition in portal veins, capillaries, and sinusoids (5). The fibrosis of liver grafts was analyzed using Masson trichromatic staining kit (Cat. No. G1346; Solarbio, Beijing, China).

Immunofluorescence

Liver graft tissues in each group were removed from recipients and cut into 8 µm slides using frozen section machine (CM1860; Leica, Wetzlar, Germany). Slides were fixed by 95% ethanol and blocked by 5% BSA for 1 hour. The following items were used as primary antibodies: mouse anti ratCD3 (150^{-1} Cat. No. SAB5500058; Sigma, USA), rabbit anti rat CD68 (100^{-1} Cat. No. GTX41868; Sigma, USA), and mouse anti rat CD86 (100^{-1} Cat. No. MA5-32078; Thermo, USA). Slides were incubated with primary antibodies respectively in a wet box at 4 ℃ for 12 hours. After washing in PBS, the following items were used as secondary antibodies for 1 hour (away from light, at room temperature): goat anti-rabbit IgG (FITC conjugated) (100^{-1} Cat. No. AP132F; Millipore, Germany), BV421 goat anti-mouse IgG (40^{-1} Cat. No. 405317; BioLegend, San Diego, CA, USA). Slides were viewed and photographed on a positive-mounted fluorescence microscope using the white light pattern (BX53F; Olympus, Japan). The primary antibody combinations were CD3 + CD68 and CD86 + CD68 to make sure that CD3 and CD86 were green and CD68 was red on fluorescence microscopy.

Transmission electron microscopy

Liver graft tissues were cut into pieces of 5 mm length and width and fixed using glutaraldehyde in phosphate buffer at 4 ℃. Then, samples were fixed by 2% Osmic acid. Samples were dehydrated by gradient alcohol and embedded in resin. Samples were stained using Prussian blue to observe and locate suspicious portal areas and small vessels. The lesion area was trimmed into small pieces. Then, samples were sliced at a thickness of approximately 70 nm. We used an H-7700 electron microscope (JEM-1400 flash; Japan) to analyze samples at 100 kV.

RNAs extraction and reverse transcription polymerase chain reaction analysis

The liver graft tissues were cut into pieces of 5 mm length and width and put into RNA later (Cat. No. R0901; Sigma, USA) for storage. The RNAs were extracted and purified using RNeasy Mini Kit (74104, Qiagen, Germantown, MD, USA). The RNAs were reverse transcribed into complementary DNA (cDNA) by All-In-One 5X RT MasterMix [G492, Applied Biological Materials (ABM), Zhenjiang, China]. Real time polymerase chain reactions (RT-PCRs) were conducted in a 20 µL reaction volume using NovoStart SYBR qPCR SuperMix Plus (E096-01A; Novoprotein, Shanghai, China). The expression of each RNA was normalized to that of β-actin, and fold changes in expression were calculated using the $2^{-\Delta\Delta Ct}$ method. The following primers were used in this study:

    IL-4: forward: GCACGAAGCTTTTGCCTGT;
    Reverse: GCATTTAGCCATGTGCCTCTG;
    IL-6: forward: CTCTGGTCTTCTGGAGTTCCG;
    Reverse: GGAAGTTGGGGGTAGGAAGGAC;
    TNF-α: forward: AGAACTCCAGGCGGTGTCT;
    Reverse: GAGCCCATTTGGGAACTTCT;
    IFN-γ: forward: GAAAGACAACCAGGCCATCA;
    Reverse: ACCTCGAACTTGGCGATG.

Western blotting

Liver graft tissues in each group were put into a homogenizer with lysis buffer (tissue 1 mg/100 µL). The lysis buffer contained radioimmunoprecipitation assay (RIPA) lysis, phenylmethylsulfonyl fluoride (PMSF; Cat. No. R0010; Solarbio, China) and Protease Inhibitor Cocktail Set I (Cat. No. 539131; Millipore, Germany) in the ratio of 100:1:1. After being lysed for 30 minutes on

ice, samples were centrifuged at 300 g. The supernatant was harvested and the concentration was detected using a bicinchoninic acid (BCA) protein concentration determination kit (Cat. No. BL521A; Biosharp, Hefei, China). The following items were used as primary antibodies: mouse anti-β-actin antibody (6,000^{-1} 42 kD Cat. No. A5441-100 μL; Sigma, USA), mouse anti-IL-10 antibody (5,000^{-1} 21 kD Cat. No. GTX632359; GeneTex, USA), HIF-1α antibody (1,000^{-1} 120 kD Cat. No. MAB5382; Millipore, Germany), rabbit anti-IL-6 antibody (2,000^{-1} 24 kD Cat. No. GTX110527; GeneTex, USA), SHP2 antibody (2,000^{-1} 68 kD Cat. No. GTX101062; GeneTex, USA), ERK1-2 antibody (10,000^{-1} 44/42 kD Cat. No. ab184699; Abcam, UK), STAT3 antibody (2,000^{-1} 88 kD Cat. No. GTX104616; GeneTex, USA), Gp130 antibody (1,000^{-1} 158 kD Cat. No. ab259927; Abcam, UK), IRF5 Antibody (1,000^{-1} 56 kD Cat. No. GTX54336; GeneTex, USA), and TGF beta 1 antibody (2,000^{-1} 44 kD Cat. No. GTX130023; GeneTex, USA). The following items were used as secondary antibodies: goat anti-rabbit IgG antibody, HRP (1,000^{-1} Cat. No. AP132P; Millipore, Germany), goat anti-Mouse IgG antibody, HRP (1,000^{-1} Cat. No. AP124P, Millipore, Germany), horseradish peroxidase (HRP) Goat anti Mouse IgG(H + I) (10,000^{-1} Cat. No. RS0001; ImmunoWay, Plano, TX, USA) and HRP goat anti-rabbit IgG(H + I) (10,000^{-1} Cat. No. RS0002, ImmunoWay, USA).

Statistical analysis

All data were presented as the mean ± standard error of mean (SEM). Comparisons between the 2 groups were performed by Student's *t*-test. Comparisons between multiple groups such as Dunnett's multiple comparisons were performed with one way analysis of variance (ANOVA). The data are displayed in graphs using the software GraphPad Prism 8.0 (GraphPad Software Inc., San Diego, CA, USA).

Results

DSA were elicited and increased C4d deposition on splenic cells in pre-sensitized liver transplant rats

At 14 days after transplantation, serum samples of the T group and TS group were collected for DSA analysis. Flow data indicated the donors' lymphocytes related IgG1, IgG2a, IgG2b, and IgG2c of sensitized rats were increased after liver transplantation (TS) compared with rats which

received liver transplantation directly (T) (*Figure 1A,1B*). On the contrary, the level of IgM was decreased in TS group compared with T group after transplantation for 14 days (*Figure 1A,1B*). This phenomenon might be related with whether major histocompatibility complex (MHC) antigens of grafts were exposed firstly or secondly in recipients. Splenic cells in each group were collected and stained with C4d to analysis C4d deposition using flow cytometry to gate lymphocytes area. Flow data indicated increased C4d deposition on splenic cells in sensitized rats with or without liver transplantation (S, TS, and TITS) compared with rats without sensitization (LEW control, T and TI) (*Figure 2A,2B*). Taken together, these results indicated that sensitization by splenic cells injection and subsequent liver transplantation elicited DSA and increased C4d deposition on splenic cells in recipients.

Sensitization was associated with accelerated dysfunction of liver graft with or without low dose of immunosuppressors

Previous studies had demonstrated that LEW rats which received liver grafts from BN rats could survive more than 100 days with less acute rejection [13-15]. In our study, weight loss, loss of appetite, and yellowing of padding could be observed in sensitized rats (TS and TITS) after the 10th to 12th day of liver transplantation, but these symptoms were rarely seen in rats without sensitization (T and TI). Thus, the blood biochemistry of rats was be analyzed because this phenomenon might be related to liver and renal dysfunction. At 14 days after transplantation, serum samples of each group were collected to detect liver and renal function including total bilirubin (TB), alanine transaminase (ALT), aspartate transaminase (AST), γ-glutamyl transpeptidase (GGT), alkaline phosphatase (ALP), and creatinine (CRE). The results showed that the liver function of the TI group was steady after the 14th day of liver transplant (*Table 1*), indicating that low dose of CsA (2 mg/kg/d) protects liver grafts from acute rejection. Indicators of TB, ALT, and AST were increased in the T group, but TB and AST were significantly lower than sensitized groups (TS and TITS) (*Table 1*). No matter if low dose of CsA was given, indicators of TB, ALT, and AST in the TS and TITS groups were increased substantially (*Table 1*) (n=3). The indicators of CRE in each group had no significant difference (*Table 1*). These data indicated that sensitization was associated with accelerated dysfunction of liver graft.

Page 6 of 18

Mang et al. AMR in a rat model of liver transplantation
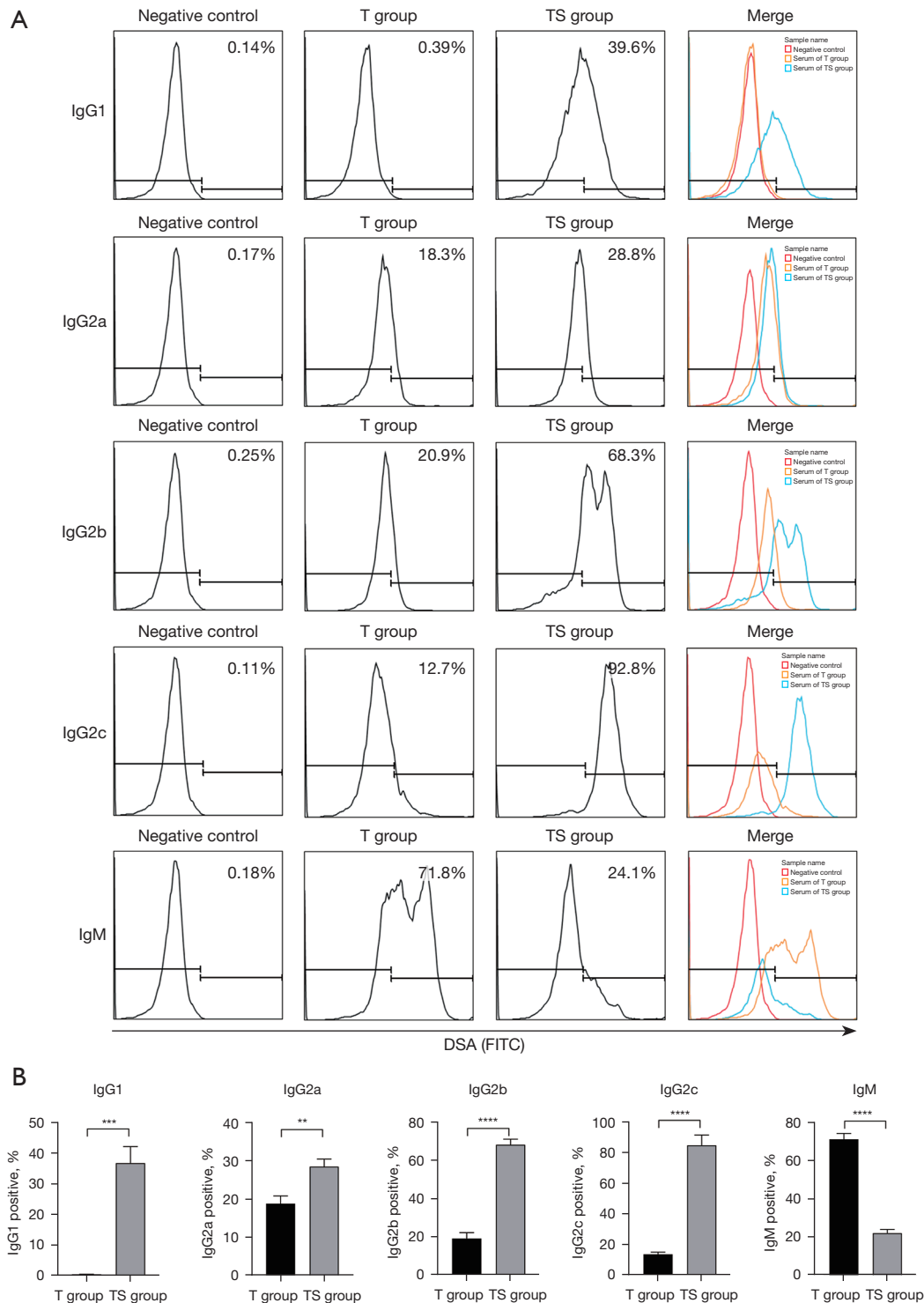
Figure 1 Levels of DSA were increased in sensitized followed transplant rats. (A) Lymphocytes of BN rats were incubated with serum of LEW rats in each group. Then secondary antibodies with FITC were used to detect DSA. (B) Flow data were presented on the statistical graph (n=3). Significant differences between each group were marked by **, P<0.01, ***, P<0.001 or ****, P<0.0001. DSA, donor-specific alloantibody; BN, Brown Norway; LEW, Lewis; FITC, fluorescein isothiocyante.
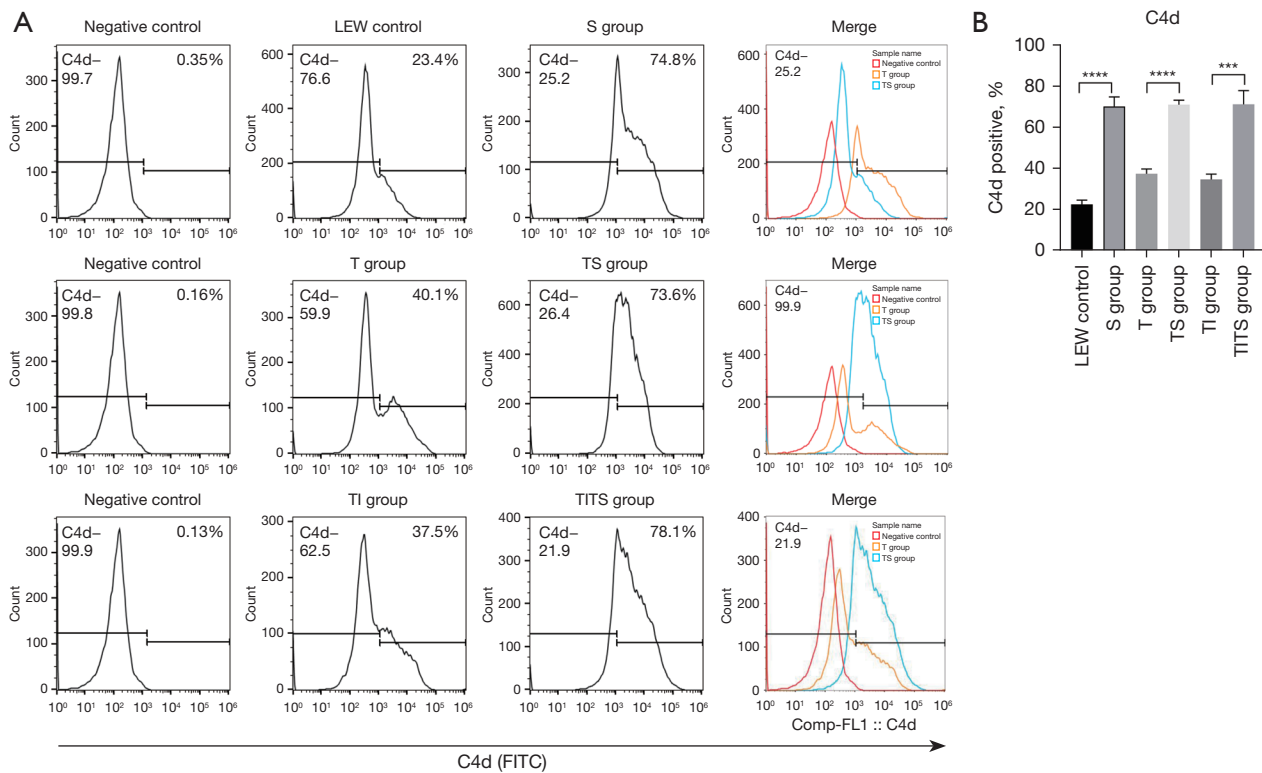
Figure 2 Levels of C4d were increased in sensitized followed transplant rats. (A) Lymphocytes of LEW rats were isolated for C4d detect using anti-C4d antibody and secondary antibody with FITC. (B) Flow data are presented on the statistical graph (n=3). Significant differences between each group were marked by ***, P<0.001, ****, P<0.0001. LEW, Lewis; FITC, fluorescein isothiocyante.

Sensitization followed by transplantation was associated with severe acute rejection and AMR

Considering the different degrees of abnormal liver function in each group (T, TS, and TITS), it was necessary to determine the presence of acute rejection. Sensitization without liver transplantation did not affect the histological structure of hepatic lobules and portal areas (*Figure 3*). In the direct liver transplantation with or without a low dose of CsA groups (T and TI), inflammatory cells such as lymphocytes were infiltrated in portal areas, and the portal areas did not or only slightly expanded. The interlobular bile duct was clearly seen with swelling epithelium and inflammatory cells infiltrated, and a few interlobular vasculitis could be observed (*Figure 3A*). The RAI for liver graft of T and TI ranged from 2 to 4 (*Table 2*). Combined with increased liver function indicators, less acute rejection might be considered in T group. In the sensitization followed by liver transplantation groups (TS and TITS), inflammatory cell infiltration was found in most or the whole area. Portal areas were enlarged, and some of the inflammatory cells in

the portal area expanded into the surrounding liver tissue (*Figure 3A*). In the TS group, it was hard to distinguish structure of interlobular arterioles, venules, and bile ducts. Even independent portal areas were difficult to find because multiple portal areas with inflammatory cell infiltrated had fused into a mass (*Figure 3A*). In the TITS group, independent portal areas and structure of interlobular arterioles, venules, and bile ducts could be still found, but these structures were badly damaged (*Figure 3A*). Different degrees of interlobular vasculitis could be observed in the TS and TITS groups (*Figure 3A*). The RAI for liver graft of TS and TITS ranged from 6 to 9 (*Table 2*) (n=3). After excluding that sensitization alone would not affect the liver structure, Sensitization followed by transplantation was associated with high RAI.

The diagnostic criteria for AMR in liver transplant was reported in 2016 (5). The diagnosis of acute AMR was related with h-(histopathology)-score and C4d-(immune)-score. The H-score evaluation was related with microvasculitis/capillaritis including number of leukocytes

　　　　　　　　Ann Transl Med 2022;10(19):1066 | https://dx.doi.org/10.21037/atm-22-4311

Page 8 of 18

Mang et al. AMR in a rat model of liver transplantation

Table 1 Accelerate liver rejection occurred in sensitized followed transplant rats

Group	TB (µmol/L)	ALT (U/L)	AST (U/L)	GGT (U/L)	ALP (U/L)	CRE (U/L)
T	61.00±2.60	143.3±13.69	322.0±26.89	14.67±3.18	473.00±66.98	25.23±3.53
TS	212.10±15.37	140.0±11.55	832.7±19.20	22.00±1.16	660.00±23.95	23.17±1.53
P value (T *vs.* TS)	***	ns	***	ns	ns	ns
TI	26.92±5.40	70.00±8.08	228.3±61.70	6.33±1.76	244.00±57.84	23.87±4.07
TITS	134.40±1.98	131.0±18.72	479.3±55.41	20.0±1.53	642.00±50.29	24.23±3.40
P value (TI *vs.* TITS)	****	*	*	**	**	ns

Data are presented as mean ± standard deviation (n=3). Serum of each group was isolated 14 days after transplant for liver and kidney function detection. Significant differences between each group were marked by ns, P>0.05; *, P<0.05; **, P<0.01; ***, P<0.001 or ****, P<0.0001. TB, total bilirubin; ALT, alanine transaminase; AST, aspartate transaminase; GGT, γ-glutamyl transpeptidase; ALP, alkaline phosphatase; CRE, creatinine.

marginated or intraluminal in the maximally which involved capillary prominent portal or sinusoids and microvascular structure (5). In our study, more than 5 leukocytes involved capillary prominent portal or sinusoid in a portal area in sensitized rats with liver transplantation (TS and TITS) (*Figure 3A*). In the most severe vessels, micro vascular disruption and filling with leukocytes could be observed in the TS group. The H-score for liver graft of TS and TITS ranged from 2 to 3 (*Table 2*). A few leukocytes were involved in capillary portal or sinusoid in rats which underwent liver transplantation without sensitization (T and TI). Dilated capillary portal or sinusoid could be observed in the T group. The H-score of liver graft of T and TI ranged from 0 to 2 (*Table 2*). For the C4d-(immune)-score, evaluation was related to whether the C4d positive deposition was more than 50% of the circumference of the vessel and ratio of vessel and sinusoids with C4d positive deposition. More than 50% interlobular venules and partial sinusoids with C4d positive deposition could be observed in TS and TITS group (*Figure 3B*). The C4d-score of liver graft of T and TI ranged from 0–1 (*Table 2*). When the C4d-score and H-score were combined, AMR was considered in rats that were pre-sensitized prior to transplantation (TS and TITS).

Interlobular bile ducts were marked using anti-cytokeratin 19 IHC staining to confirm the degree of interlobular bile duct damage. Interlobular bile ducts were stained brown with complete structure in LEW control, S, T, and TI groups. In the T and TI groups, interlobular bile ducts were dilated with edematous biliary epithelial cells. However, quite a lot of interlobular bile ducts were stained brown with incomplete structure in sensitized rats (TS and TITS groups). In the TS group, the interlobular bile ducts were barely visible, which was replaced by scattered biliary epithelial cells with brown stain (*Figure 4A*). These data showed that sensitization followed by transplantation was associated with severe biliary epithelial damage. Combined with increased liver function indicators, severe acute rejection was considered possible in the T group. After excluding that sensitization alone would not affect the liver, sensitization followed by transplantation was associated with severe acute rejection.

Liver graft fibrosis was evaluated by Masson staining. Red hepatocytes and few blue interstitial tissue of portal areas were seen in recipients without sensitization and control groups (LEW control, S, T, and TI groups). In sensitization followed by transplantation rats (TS and TITS groups), turquoise or blue interstitial areas were significantly outward spreading. Several portal areas had fused together and were stained with turquoise or blue in TS group (*Figure 4B*). These data showed sensitization followed by transplantation might be associated with severe fibrosis. However, severe fibrosis needed to be confirmed by further ultra microstructure study to find if more collagenous fibers were deposited in space of tissue compared with non-sensitization groups.

The CD20 B cells infiltration was observed in an AMR case. Anti-CD20 monoclonal antibody is one of the most important methods to treat AMR in ABO compatible/incompatible liver transplantation (16,17). To identify if infiltrated lymphocytes contained CD20 B cells, anti-CD20 IHC staining was used in liver graft slides. The results showed that portal areas of rats with sensitization followed by liver transplantation (TS and TITS groups) were infiltrated with CD20 B cells. Sensitization alone did not increase the number of CD20 B cells recruited. Compared
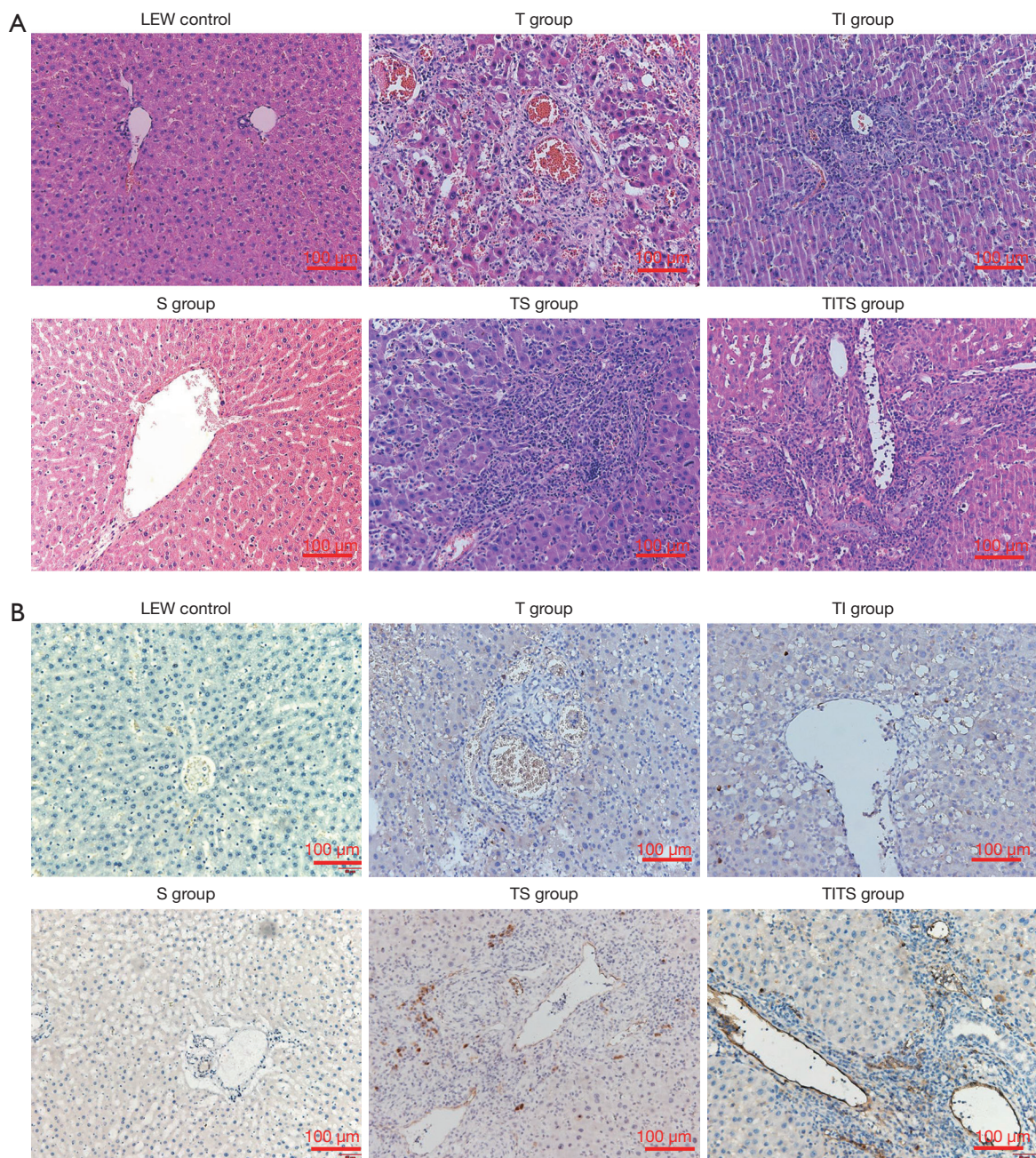
Figure 3 Accelerate liver rejection and C4d deposition occurred in sensitized followed transplant rats. (A) Inflammation of portal areas, bile ducts, vascular endothelium, and capillaries is shown by HE staining in each group. (B) C4d deposition is shown in IHC. LEW, Lewis; HE, hematoxylin and eosin; IHC, immunohistochemistry.

with the sensitization followed by liver transplantation groups, few infiltrated CD20 B cells were seen in rats with transplantation alone (T and TI groups), suggesting that sensitization followed by transplantation resulted recruitment of CD20 B cells to liver graft (*Figure 4C*).

Hyperphagocytosis of Kupffer cells and capillary inflammation were observed under transmission electron microscope (TEM)

Observation under TEM might be helpful to reveal capillary inflammation, base membrane, and substructure change in

Page 10 of 18

Mang et al. AMR in a rat model of liver transplantation

Table 2 AMR was occurred in sensitized followed transplant rats

Group	RAI	Portal Inflammation	Bile duct damage	Venular endothelialitis	H-score	C4d-score
C	0.00±0.00	0.00±0.00	0.00±0.00	0.00±0.00	0.00±0.00	0.00±0.00
S	0.00±0.00	0.00±0.00	0.00±0.00	0.00±0.00	0.00±0.00	0.00±0.00
T	4.00±0.00	1.67±0.33	1.33±0.33	1.00±0.00	1.33±0.33	0.33±0.33
TS	8.00±0.57	2.67±0.33	3.00±0.00	2.33±0.33	2.67±0.33	2.67±0.33
P value (T *vs.* TS)	**	**	**	*	*	**
TI	2.67±0.33	0.67±0.33	1.00±0.00	1.00±0.00	0.67±0.33	0.00±0.00
TITS	6.67±0.88	2.33±0.33	2.67±0.33	1.67±0.33	2.33±0.33	2.33±0.33
P value (TI *vs.* TITS)	*	*	**	–	*	**

Data are presented as mean ± standard deviation (n=3). RAI score, histopathology score and C4d score were evaluated according to HE staining and IHC. *, P<0.05; **, P<0.01. AMR, antibody-mediated rejection; HE, hematoxylin and eosin; IHC, immunohistochemistry. RAI: rejection activity index; H-score: histopathology-score.

a pre-sensitized followed by transplant model. However, inflammation levels in different portal areas were different, which complicated the capacity to describe common characteristics of AMR in liver transplantation. In our study, we choose a typical rejection area in the pre-sensitized followed by transplant group for observation under TEM. The purpose was to find characteristics or evidence of AMR. In our study, the junctions between epithelial cells of the bile duct were widened in the pre-sensitized followed by transplant rats (TS group). The villi of bile duct epithelium had disappeared. However, the villi of bile ducts' epithelium were visible, and no widened junctions were observed in the direct transplant group (T group). Kupffer cells, macrophages, and lymphocytes were filled with hepatic sinus in the TS group. Phagocytic vesicles were easily observable in most Kupffer cells. This phenomenon was not seen in the T group; although Kupffer cells could be seen in the T group, no obvious phagocytic vesicles were observed (*Figure 5*).

M1 phenotype macrophagocytes were activated in the sensitization-induced AMR rat model

We detected CD3 and CD68 using immunofluorescence to determine whether severe rejection of AMR models was related with T cells and monocytes. The results showed that the CD3 T cells infiltration (green immunofluorescence) increased in liver grafts without immunosuppressors (T) compared with the TI group. However, liver grafts of sensitized rats with immunosuppressors (TITS) were infiltrated with more CD3 T cells compared with the TI group. The phenomenon might be caused by macrophages

recruitment (CD68 monocyte–macrophages, red immunofluorescence) which was related with complement fixed ability of DSA in sensitized rats (TS and TITS groups). Macrophages recruitment was not seen in grafts of rats without sensitization. Considering that more severe rejection was observed in sensitization followed liver transplantation (TS and TITS groups), we studied the phenotype of infiltrated monocyte–macrophages using anti-CD86 (surface marker of M1 phenotype macrophages, green immunofluorescence) and anti-CD68. The results showed that most infiltrated macrophages (red immunofluorescence) expressed CD86 (green immunofluorescence), which suggested that macrophages recruitment in liver grafts of sensitized rats (TS and TITS groups) might be specific to the M1 phenotype (*Figure 6*). To further confirm if macrophages recruited into liver grafts were converted to M1 phenotype in sensitization-related AMR animal models, cytokines and transcription factors which were related with transformation and maintenance of M1 macrophage phenotype were detected by western blotting. The results showed that the levels of IL-10 and transforming growth factor (TGF)-β decreased and that of IL-6 increased in the sensitized groups (TS and TITS groups) compared with the direct transplantation groups (T and TI groups). Nuclear factor (NF)-κB, HIF-α, and IRF5, which could contribute to inflammation and M1 phenotype macrophages maintenance, were increased in the sensitized groups (TS and TITS groups) (*Figure 7*). These data showed that severe rejection of the pre-sensitized groups might be related to macrophages recruitment with M1 phenotype conversion.
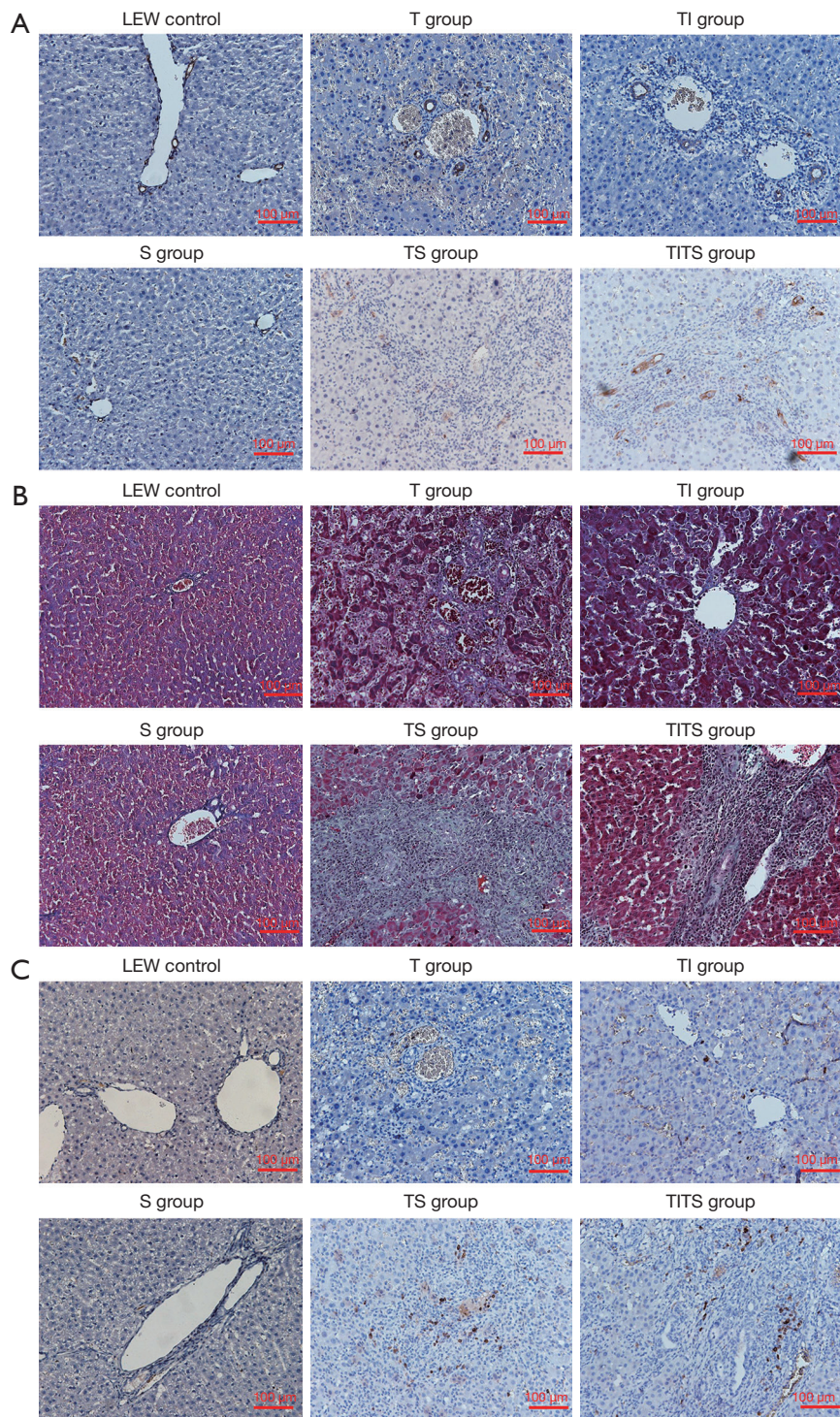
Figure 4 Severe interlobular bile ducts injury, fibrosis, and CD20 cells infiltration were observed in pre-sensitized followed by transplant rats. (A) Interlobular bile ducts were marked by CK19 in each group by IHC staining. (B) Degree of fibrosis was detected by Masson staining. (C) CD20 B cells were marked in each group by IHC staining. LEW, Lewis; IHC, immunohistochemistry.

Page 12 of 18

Mang et al. AMR in a rat model of liver transplantation
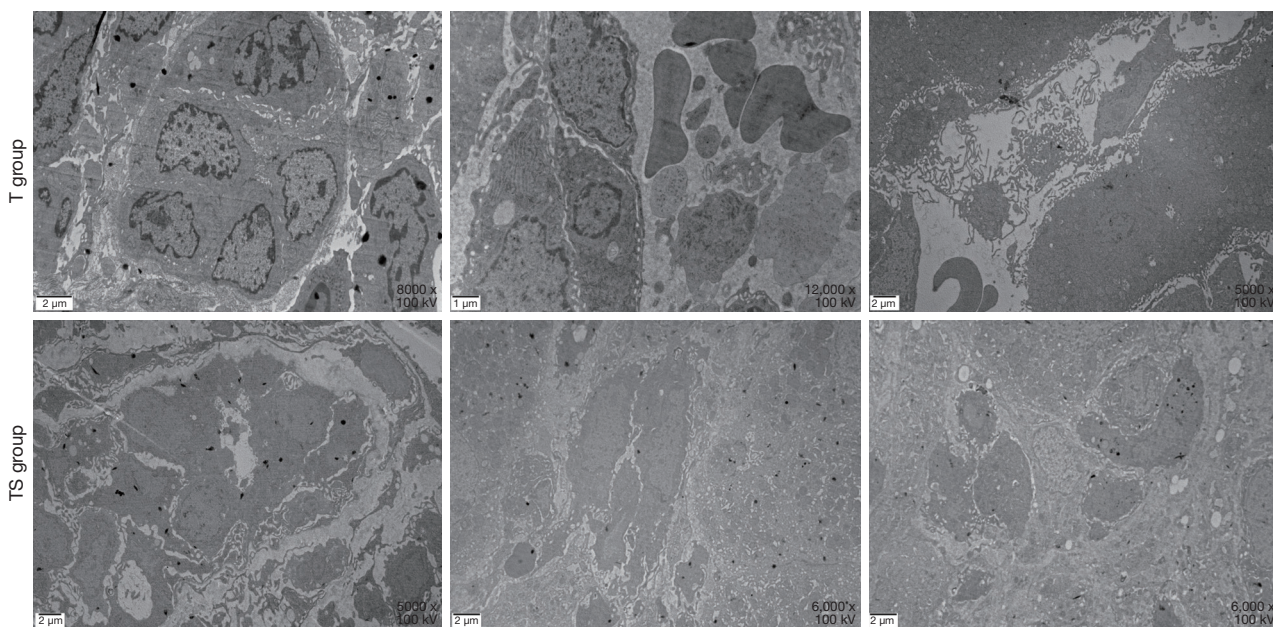
Figure 5 Hyperphagocytosis of Kupffer cells and capillary inflammation were observed under TEM in pre-sensitized followed by transplant rats. TEM, transmission electron microscope.
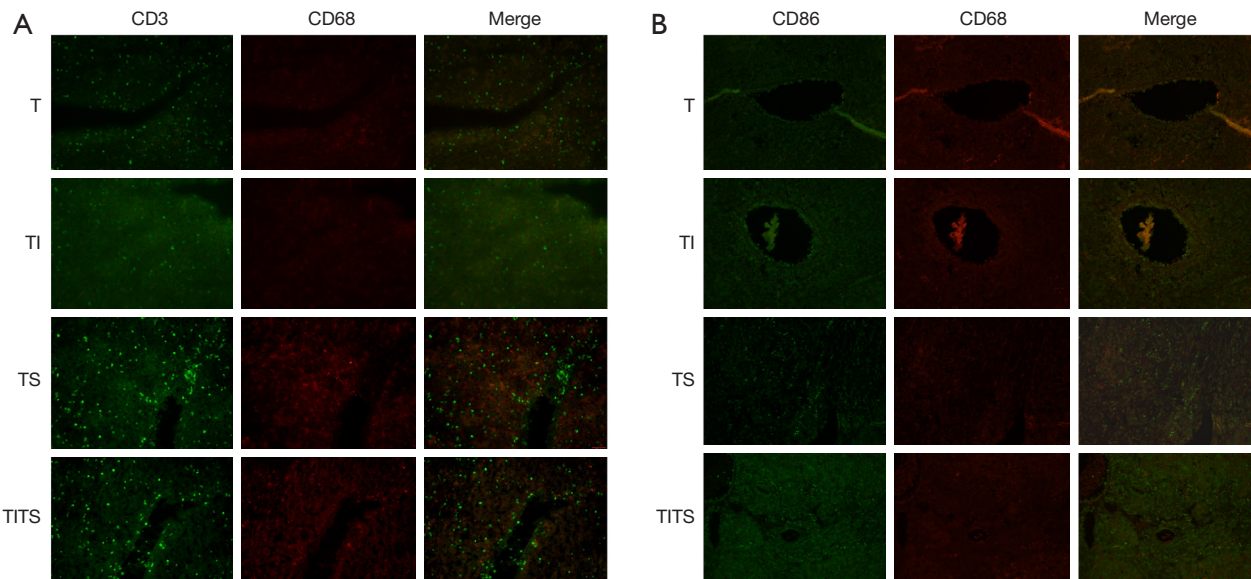
Figure 6 M1 phenotype macrophagocytes were activated in sensitization induced AMR rat model. (A) CD3 cells were marked as green and CD68 cells were marked as red. (B) CD86 cells were marked as green and CD68 cells were marked as red. By immunofluorescence. Magnification times 400×. AMR, antibody-mediated rejection.

IL-6-related signaling pathway was activated in the sensitization-induced AMR rat model

Cytokine profiles of liver grafts were evaluated by detecting IL-6, interferon (IFN)-γ, IL-4, and tumor necrosis factor (TNF)-α. The results showed that sensitization followed by transplantation or severe rejection induced increasing of IL-6, IL-4, IFN-γ, and TNF-α. These cytokine levels were
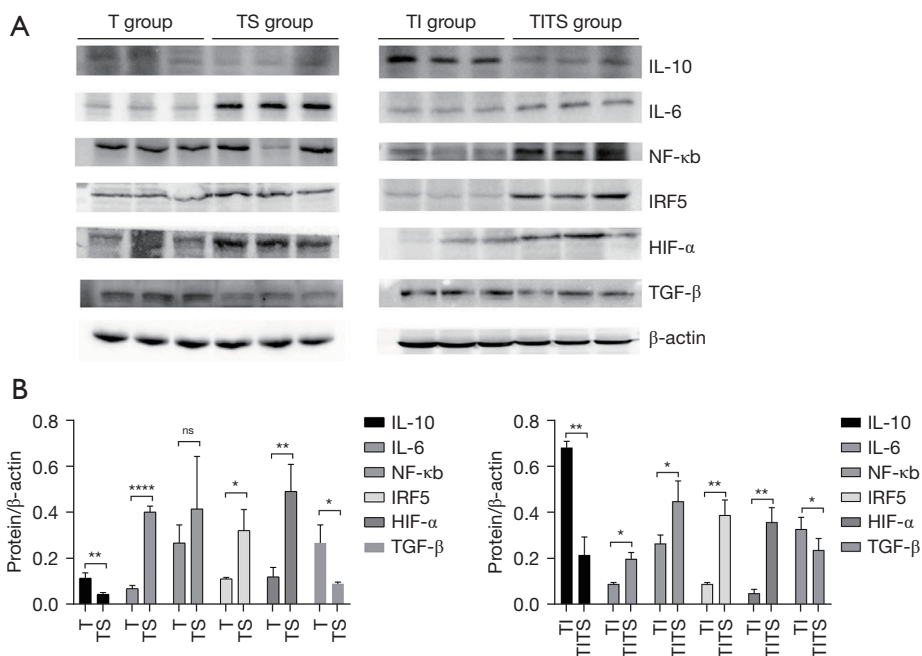
Figure 7 Cytokines and transcription factors which were related with transformation and maintenance of M1 macrophage phenotype were increased in pre-sensitized followed by transplant rats. (A) IL-10, IL-6, NF-κb, IRF5, HIF-α, and TGF-β were detected in each group. (B) WB data were analyzed by Image J and presented on the statistical graph (n=3). Significant differences between each group were marked by [ns], P>0.05; *, P<0.05; **, P<0.01 or ****, P<0.0001. WB, Western blotting; IL-10, interleukin-10; IL-6, interleukin-6
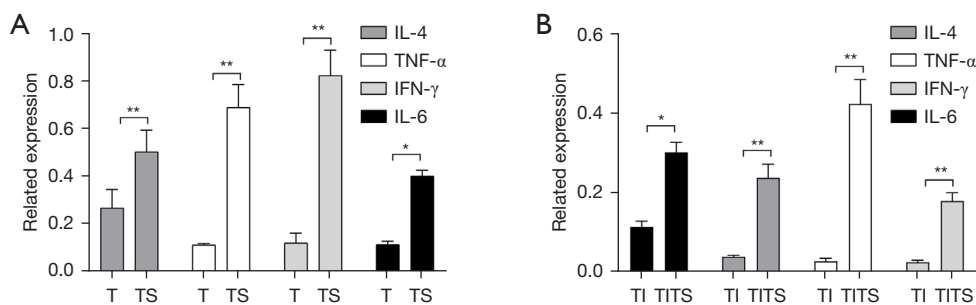
Figure 8 Sensitized followed transplantation induced increasing of IL-6, IL-4, IFN-γ, and TNF-α. Significant differences between each group were marked by *, P<0.05 or **, P<0.01. IL-6, interleukin-6; IL-4, interleukin-4; IFN-γ, interferon-γ; TNF-α, tumor necrosis factor-α.

lowest in the grafts of direct transplantation with low dose immunosuppression group. These data showed that severe rejection might be related to increased cytokines including IL-6, IL-4, IFN-γ, and TNF-α (*Figure 8*).

To further explore altered cytokines-related factors in AMR rat models, the levels of gp130, JAK1, STAT3, SHP2, and ERK1-2 were assessed by western blotting because these factors were related with increased binding to high endothelial venule (18) or inflammation (19,20).

An important component of the IL-6 receptor, Gp130, remained unchanged in each transplantation group. However, downstream signaling pathways which were related with IL-6-gp130 complex activation might have been activated by sensitization followed by transplantation. The results showed that JAK1, STAT3, SHP2, and ERK1-2 were up-regulated in the sensitization followed by transplantation groups (TS and TITS) compared with the direct transplantation groups (T and TI). Both STAT3

Ann Transl Med 2022;10(19):1066 | https://dx.doi.org/10.21037/atm-22-4311
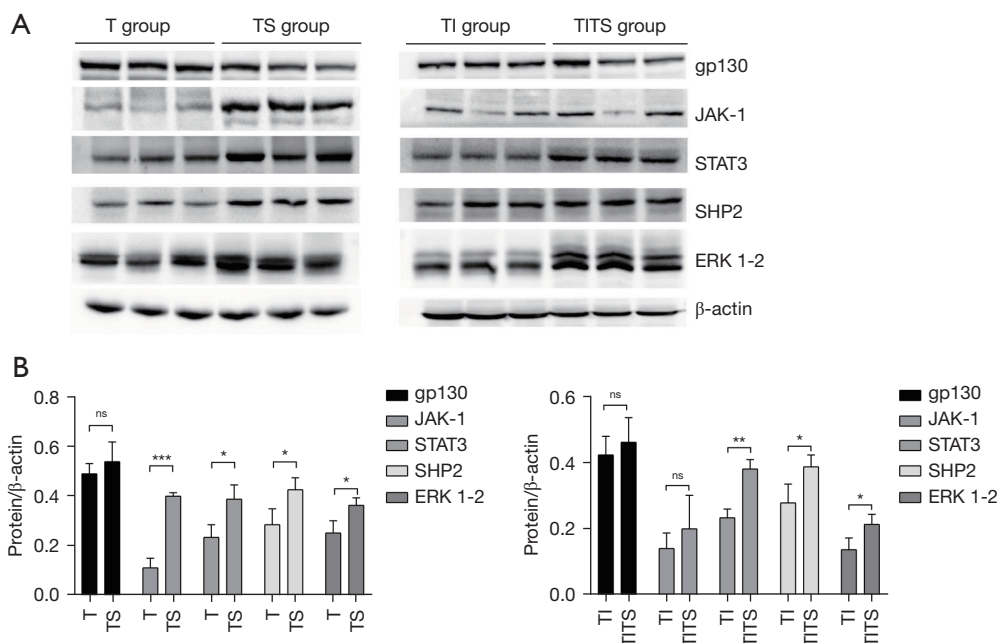
Figure 9 The IL-6 signaling pathway was activated in sensitization induced AMR rat model. (A) gp130, JAK-1, STAT3, SHP2, and ERK1-2 were detected in each group. (B) WB data were analyzed by ImageJ and presented on the statistical graph (n=3). Significant differences between each group were marked by [ns], $P>0.05$; *, $P<0.05$; **, $P<0.01$ or ***, $P<0.001$. AMR, antibody-mediated rejection; WB, Western blot.

and ERK1-2 were predominant targets of IL-6 signaling (*Figure 9*). By combined analysis of IL-6 upregulation in the pre-sensitization followed by transplantation groups, the data showed that IL-6 signaling might be activated in sensitization-induced AMR rat model.

Discussion

In recent years, AMR in liver transplantation has received more attention because several graft dysfunction cases of unknown reason have been considered AMR (1,2). Besides, donor recipients with AMR (especially AMR-related with *de novo* DSA) have a poor prognosis (1). Subsequently, the terminology of guidelines was updated (humoral rejection to AMR and plasma cell hepatitis to plasma cell rich–rejection), along with the specified diagnostic criteria of AMR (5). At present, the diagnosis of AMR can abide by following criteria: (I) histology: endothelial cell hypertrophy, portal capillary dilatation, microvasculitis with monocytes, eosinophils and neutrophils, and portal/peri-portal oedema—microvascular involvement of the central veins; (II) elevated DSAs; (III) diffuse C4d deposition of microvasculature; (IV) exclusion of other liver diseases or complications. No consensus exists on the optimal treatment of liver AMR, some of them using

KT therapeutic regimen (21). However, microvascular inflammation, endothelial cell activation by electron microscopy, gene expression profile, and therapeutic trials design required further exploration. Meanwhile, molecular mismatch also needs to be taken into consideration, for it has been reported that molecular mismatch can predict T Cell-mediated rejection and *de novo* donor-specific antibody formation after living donor liver transplantation (22). Thus, an animal liver transplantation model with AMR is necessary to explore the mechanism of AMR. It also helps to elucidate the circumstances in which the liver graft is intolerant to DSA. Transplantation models with AMR in rats have been reported previously (23). An opinion is that reduced-size liver allografts bear an increased risk of AMR which might be related to the dysfunction of Kupffer cells (23). Another opinion is that AMR occurs in liver transplantation rat models with chronic rejection (24). However, reports about standard acute AMR models in liver transplantation rats are scarce. A possible solid organ transplant rat model which might be related to DSA and AMR is pre-sensitized rats as recipients (10). Accelerated rejection occurred in pre-sensitized recipients which underwent skin transplant followed by heart transplant or transfusion followed by kidney transplant (10,25,26). Evidence of endothelial injury

and complement activation were observed in these animal models. Thus, we hypothesize that accelerated rejection in pre-sensitized followed by liver transplantation might be related to AMR. Liver transplant (BN to LEW rat) models were used to confirm that recipients could survive more than 100 days with reduced or without immunosuppression (14). In our study, high level DSA and accelerated rejection were observed in pre-sensitized followed by transplantation with low dose of CsA.

The HE analysis indicated that the pre-sensitized followed by liver transplantation group a had higher RAI compared with the direct transplant group. Severe injury of the bile ducts and small interlobular vessels were observed in pre-sensitized followed by transplantation groups. This phenomenon might be related to inflammation associated with endothelial injury. The most important characteristic of AMR in solid organs is endothelial injury (2,4,5,27). Thus, evidence of endothelial injury was required to confirm the establishment of a suitable pre-sensitization followed by transplantation rat model. Lymphocytes or monocytes infiltration in blood capillary pre bile ducts could be observed in pre-sensitized followed by transplantation rats. Even destruction of blood capillaries could be observed. Although bile duct edema and lymphocytes infiltration were observed in direct transplant rats, obvious destruction of capillary structure and lymphocytes infiltration were not observed. This means that more serious capillary inflammation occurred in the pre-sensitized followed by transplantation rat models. The vascular endothelium is a target of activated antibody-complement. Therefore, sinusoidal lesions need to be considered. Under the TEM, monocytes and lymphocytes filled the hepatic sinus. Disappearance of the villi of biliary epithelial cells was also observed in pre-sensitized followed by transplantation rats. This phenomenon was hard to find in direct transplantation rats. The deposition of electron dense material and damage of base film were not observed under TEM. This might be related to the large space between the endothelial cells of the hepatic sinusoids. Conversely, it is difficult to find common characteristics under TEM because the degree of lesions was different in different portal areas. Some special or small lesions are difficult to locate under TEM. Our study showed positive C4d staining in interlobular veins and sinuses and mononuclear macrophages recruitment (especially M1 macrophages). Complement activation is closely related to macrophage recruitment (10). The M1 macrophages play an important role in pro-inflammatory processes (28,29). Antibody-related phagocytosis of Kupffer cells plays an important role in liver allograft resistance

to DSA-mediated injury (2). In the pre-sensitized models, Kupffer cells containing numerous phagocytic vesicles were easy to find. Pre-sensitized models and Kupffer cells replacement (30) might help to explore whether Kupffer cells participate in AMR. Severe fibrosis around the portal area is one of features of AMR in liver transplant (5,31). This kind of fibrosis occurs not only in chronic rejections (32), but also in acute AMR, as increased fibrin (31). The progression of fibrosis in pre-sensitized followed by transplantation rats was surprising to us. Within 2 weeks after transplantation, extensive fibrosis occurred around the portal areas, which was significantly different from the direct transplantation groups. The TEM showed that fibrosis was more extensive because large number of collagen fibers were found in the Disse space in pre-sensitized followed by transplantation rats. By combining these data together, our study demonstrated that characteristics of rejection in pre-sensitized followed by transplantation rats were different from directly transplanted rats. These characteristics are mainly shown as a high level of DSA, accelerated and severe rejection, extensive fibrosis progression, endothelial injury (especially capillary inflammation), complement activation, macrophage recruitment (M1 macrophages transfer), and Kupffer cells filled with phagosomes. These characteristics made it possible to use pre-sensitized followed by transplantation rats as acute AMR models to explore the mechanism and potential therapy.

We observed M1 macrophages conversion, vascular endothelial cells injury, and lymphocytes binding (capillary inflammation) in sensitized rat models, which might have been related to accelerate rejection. The mechanisms of M1 macrophages conversion and capillary inflammation were closely related to IL-6 signaling pathway activity (18,33,34). Activation of the IL-6 signaling pathway is involved in inflammation (35), adaptive cellular immunity (36), and fibrosis (37), which finally contributes to allograft injury (38). Clinical and preclinical studies have indicated that IL-6 is involved in acute rejection after liver transplant (39,40). A previous study has shown that IL-6 gene polymorphisms are predictive of acute rejection following clinical liver transplantation (40). Another rodent study showed that pretreatment of recipient rats with IL-6 *in vivo* 24 and 12 h before surgery promoted donor liver regeneration and improved the survival rate after partial liver transplantation (41). The classical IL-6 signaling pathway indicates that IL-6 binds to the membrane of IL-6R. The IL-6/IL-6R complex binds to gp130, inducing dimerization and initiation of signaling (18). Activation of gp130 in

Page 16 of 18

Mang et al. AMR in a rat model of liver transplantation

lymphocytes leads to activation of JAK kinases resulting in gp130 phosphorylation on tyrosine residues (18). This leads to STAT3 recruitment and activation, which is involved in antiapoptotic responses via bcl-2 and bcl-xL induction (18,42). Activation of the MEK-1 and ERK1-2 pathway leads to enhanced interaction of the cytoplasmic portion of L-selectin and components of the cytoskeleton, which leads enhanced L-selectin-mediated adhesion to high endothelial venules (18,43). As a regulator, SHP2 could ensure the signaling robustness and information transfer of IL-6 (19). Our study showed that IL-6 was increased in pre-sensitized followed by transplant rats. Moreover, genes related to the IL-6 signaling pathway such as STAT3, SHP2, and ERK1-2 were changed in sensitized followed by transplant rats. By combining the factor of accelerated rejection in sensitized followed by transplant rats, our data indicated that the IL-6 signaling pathway might be involved in liver graft rejection. Further study using therapeutants such as dissociative protein sgp130 (competitively bind to IL-6) or tocilizumab could demonstrate existence and related therapy of the IL-6 signaling pathway and AMR in sensitized followed by transplant rat models. In our model, we explored the mechanism of AMR in liver graft from the point of view of immune microenvironment. Immune response plays an important role in the process of inflammatory response. By constructing the AMR rat model, we observed the M1 macrophages conversion and the activation of IL-6 signaling, indicating the potential mechanism of AMR from a new perspective.

Conclusions

High levels of DSA and accelerated liver rejection occurred in sensitized followed by liver transplant rat models with or without low dose immunosuppressors using BN rats as donors and LEW rats as recipients. Accelerate liver rejection in these models has characteristics such as endothelial injury, capillary inflammation, C4d deposition, and M1 macrophages recruitment. Potential mechanisms might be activation of the IL-6 signaling pathway. Pre-sensitized followed by liver transplant rats might be potential AMR models for further study.

Acknowledgments

Footnote

References

1. Vionnet J, Sempoux C, Pascual M, et al. Donor-specific antibodies in liver transplantation. Gastroenterol Hepatol

2020;43:34-45.

2. Taner T, Stegall MD, Heimbach JK. Antibody-mediated rejection in liver transplantation: current controversies and future directions. Liver Transpl 2014;20:514-27.

3. Youn JC, Zhang X, Nishihara K, et al. Post-transplantation outcomes of sensitized patients receiving durable mechanical circulatory support. J Heart Lung Transplant 2022;41:365-72.

4. Petty M. Antibody-Mediated Rejection in Solid Organ Transplant. AACN Adv Crit Care 2016;27:316-23.

5. Demetris AJ, Bellamy C, Hübscher SG, et al. 2016 Comprehensive Update of the Banff Working Group on Liver Allograft Pathology: Introduction of Antibody-Mediated Rejection. Am J Transplant 2016;16:2816-35.

6. Hogen R, DiNorcia J, Dhanireddy K. Antibody-mediated rejection: what is the clinical relevance? Curr Opin Organ Transplant 2017;22:97-104.

7. Del Bello A, Congy-Jolivet N, Danjoux M, et al. De novo donor-specific anti-HLA antibodies mediated rejection in liver-transplant patients. Transpl Int 2015;28:1371-82.

8. Maurice JB, Nwaogu A, Gouda M, et al. Acute Antibody-mediated rejection in liver transplantation: Impact and applicability of the Banff working group on liver allograft pathology 2016 criteria. Hum Pathol 2022;127:67-77.

9. Sakamoto S, Akamatsu N, Hasegawa K, et al. The efficacy of rituximab treatment for antibody-mediated rejection in liver transplantation: A retrospective Japanese nationwide study. Hepatol Res 2021;51:990-9.

10. Huang G, Wilson NA, Reese SR, et al. Characterization of transfusion-elicited acute antibody-mediated rejection in a rat model of kidney transplantation. Am J Transplant 2014;14:1061-72.

11. He L, Dono K, Gotoh M, et al. Role of the liver in alloimmune response following inoculation of donor spleen cells. Cell Transplant 2,000;9:725-8.

12. Banff schema for grading liver allograft rejection: an international consensus document. Hepatology 1997;25:658-63.

13. Zimmermann FA, Davies HS, Knoll PP, et al. Orthotopic liver allografts in the rat. The influence of strain combination on the fate of the graft. Transplantation 1984;37:406-10.

14. Li J, Lai X, Liao W, et al. The dynamic changes of Th17/Treg cytokines in rat liver transplant rejection and tolerance. Int Immunopharmacol 2011;11:962-7.

15. Murase N, Starzl TE, Tanabe M, et al. Variable chimerism, graft-versus-host disease, and tolerance after different kinds of cell and whole organ transplantation from Lewis to brown Norway rats. Transplantation 1995;60:158-71.

16. Kim BW, Park YK, Kim YB, et al. Effects and problems of adult ABO-incompatible living donor liver transplantation using protocol of plasma exchange, intra-arterial infusion therapy, and anti-CD20 monoclonal antibody without splenectomy: case reports of initial experiences and results in Korea. Transplant Proc 2008;40:3772-7.

17. Kanazawa H, Fukuda A, Mali VP, et al. Chemotherapy-induced B-cell depletion in hepatoblastoma patients undergoing ABO-incompatible living donor liver transplantation. Pediatr Transplant 2016;20:401-7.

18. Rose-John S, Neurath MF. IL-6 trans-signaling: the heat is on. Immunity 2004;20:2-4.

19. Fiebelkow J, Guendel A, Guendel B, et al. The tyrosine phosphatase SHP2 increases robustness and information transfer within IL-6-induced JAK/STAT signalling. Cell Commun Signal 2021;19:94.

20. Miller CL, Madsen JC. IL-6 Directed Therapy in Transplantation. Curr Transplant Rep 2021;8:191-204.

21. Lee BT, Fiel MI, Schiano TD. Antibody-mediated rejection of the liver allograft: An update and a clinico-pathological perspective. J Hepatol 2021;75:1203-16.

22. Ono K, Ide K, Tanaka Y, et al. Molecular Mismatch Predicts T Cell-Mediated Rejection and De Novo Donor-Specific Antibody Formation After Living Donor Liver Transplantation. Liver Transpl 2021;27:1592-602.

23. Astarcioglu I, Cursio R, Reynes M, et al. Increased risk of antibody-mediated rejection of reduced-size liver allografts. J Surg Res 1999;87:258-62.

24. Wan R, Ying W, Zeng L, et al. Antibody-mediated response in rat liver chronic rejection. Transplant Proc 2011;43:1976-9.

25. Ueda H, Itoh S, Iwamoto Y, et al. Sensitization interval and administration method alter the effect of 15-deoxyspergualin on heart transplantation in sensitized recipient rats. Transpl Int 1996;9:551-6.

26. Stadlbauer TH, Faske R, Heidt MC, et al. Apoptotic cell death during accelerated rejection in sensitized rat recipients of cardiac allografts. Transplant Proc 2009;41:2621-4.

27. Drachenberg CB, Papadimitriou JC. Endothelial injury in renal antibody-mediated allograft rejection: a schematic view based on pathogenesis. Transplantation 2013;95:1073-83.

28. Liu Y, Pu X, Qin X, et al. Neutrophil Extracellular Traps Regulate HMGB1 Translocation and Kupffer Cell M1 Polarization During Acute Liver Transplantation Rejection. Front Immunol 2022;13:823511.

29. Yao Y, Xu XH, Jin L. Macrophage Polarization in Physiological and Pathological Pregnancy. Front Immunol 2019;10:792.

30. Endo K, Hori T, Jobara K, et al. Pretransplant replacement of donor liver grafts with recipient Kupffer cells attenuates liver graft rejection in rats. J Gastroenterol Hepatol 2015;30:944-51.

31. Kunugi S, Shimizu A, Ishii E, et al. The pathological characteristics of acute antibody-mediated rejection in DA-to-Lewis rat orthotopic liver transplantation. Transplant Proc 2011;43:2737-40.

32. Shimizu A, Ishii E, Kuwahara N, et al. Chronic antibody-mediated responses may mediate chronic rejection in rat orthotopic liver transplantation. Transplant Proc 2013;45:1743-7.

33. Kawashima T, Murata K, Akira S, et al. STAT5 induces macrophage differentiation of M1 leukemia cells through activation of IL-6 production mediated by NF-kappaB p65. J Immunol 2001;167:3652-60.

34. Chen X, Fu E, Lou H, et al. IL-6 induced M1 type macrophage polarization increases radiosensitivity in HPV positive head and neck cancer. Cancer Lett 2019;456:69-79.

35. Uehara M, Solhjou Z, Banouni N, et al. Ischemia augments alloimmune injury through IL-6-driven CD4+ alloreactivity. Sci Rep 2018;8:2461.

36. von Rossum A, Rey K, Enns W, et al. Graft-Derived IL-6 Amplifies Proliferation and Survival of Effector T Cells That Drive Alloimmune-Mediated Vascular Rejection. Transplantation 2016;100:2332-41.

37. Kang S, Tanaka T, Kishimoto T. Therapeutic uses of anti-interleukin-6 receptor antibody. Int Immunol 2015;27:21-9.

38. Verleden SE, Martens A, Ordies S, et al. Immediate post-operative broncho-alveolar lavage IL-6 and IL-8 are associated with early outcomes after lung transplantation. Clin Transplant 2018;32:e13219.

39. Yao J, Feng XW, Yu XB, et al. Recipient IL-6-572C/G genotype is associated with reduced incidence of acute rejection following liver transplantation. J Int Med Res 2013;41:356-64.

40. Karimi MH, Daneshmandi S, Pourfathollah AA, et al. Association of IL-6 promoter and IFN-γ gene polymorphisms with acute rejection of liver transplantation. Mol Biol Rep 2011;38:4437-43.

41. Selzner N, Selzner M, Tian Y, et al. Cold ischemia decreases liver regeneration after partial liver transplantation in the rat: A TNF-alpha/IL-6-dependent mechanism. Hepatology 2002;36:812-8.

42. Chen X, Han K, Lin G, et al. Ctenopharyngodon Idella STAT3 alleviates autophagy by up-regulating BCL-2 expression. Fish Shellfish Immunol 2019;91:194-201.

43. Kirveskari J, Paavonen T, Häyry P, et al. De novo induction of endothelial L-selectin ligands during kidney allograft rejection. J Am Soc Nephrol 2,000;11:2358-65.

(English Language Editor: J. Jones)